

# We are IntechOpen, the world's leading publisher of Open Access books Built by scientists, for scientists

**4,800**

Open access books available

**122,000**

International authors and editors

**135M**

Downloads

Our authors are among the

**154**

Countries delivered to

**TOP 1%**

most cited scientists

**12.2%**

Contributors from top 500 universities



**WEB OF SCIENCE™**

Selection of our books indexed in the Book Citation Index  
in Web of Science™ Core Collection (BKCI)

Interested in publishing with us?  
Contact [book.department@intechopen.com](mailto:book.department@intechopen.com)

Numbers displayed above are based on latest data collected.

For more information visit [www.intechopen.com](http://www.intechopen.com)



# Thermal Conductivity Improvement of PEEK/ZrO<sub>2</sub> Coated MWCNT Nanocomposites

Kaushik Pal and Jin Kuk Kim

*Polymer Science and Engineering,  
School of Nano and Advanced Materials Engineering,  
Gyeongsang National University,  
Republic of Korea*

## 1. Introduction

Since the landmark paper on carbon nanotubes (CNTs) by Iijima in 1991[1], carbon nanotubes have been an attractive materials for fundamental research studies and become one of the most important materials in the 21<sup>st</sup> century technology. Several applications were proposed for carbon nanotubes many of which are concerned with conductive or high strength composites [2,3], in which the inclusion of carbon nanotubes in a ceramic matrix is expected to produce composites possessing high stiffness and improved mechanical properties compared to the single phase ceramic material [4] and already been used as nano probes, gas storage containers, nanoelectronic devices, sensors, composite reinforcements, and integrated interconnection due to their extraordinary properties [5-8]. Currently, there has been widespread interest in the fabrication of one-dimensional nano scale materials by filling or coating CNT with various kinds of materials including metals (such as zirconium oxide, hafnium oxide, aluminum oxide, and conductive materials such as gold, copper, and platinum), non-metals, carbides, and oxides which possess distinctive chemical [9-13], mechanical, and physical properties [14-16].

Zirconia (ZrO<sub>2</sub>), especially in the powder form, is very attractive material applied in a wide variety of technological fields such as catalysts, oxygen sensors, fuel cells, optical devices, and electronic devices [17-20]. Several preparation methods have also been reported on the synthesis of ZrO<sub>2</sub>; including chemical vapor deposition, spray pyrolysis, ion sputtering, sol-gel, and chemical precipitation [21-24]. This mainly results from its excellent properties including thermal, chemical, and mechanical stability as well as unique optical and dielectric properties.

Carbon nanotubes are widely used in composite materials because CNTs have excellent electrical and thermal properties [25-28], because, a change in structure and properties by diameter, bonding structure, rope structure of carbon nanotube. In contrast, the polymers typically ~ 0.2W/mK has low thermal conductivity. But the rapid development of the electronics industry to emit more heat and small electronic components can be used in polymer materials of high thermal conductivity is required. Temperature rises 10 °C has been reported lost half-life of electronic devices. Therefore, effectively it is important to release heat quickly from electronic components. To develop heat emission high polymer, if

we use the high thermal conductivity of carbon nanotube, thermal conductivity of the polymer can be improved.

Poly (ether ether ketone) (PEEK) is a semi-cystalline thermoplastic polymer with superior mechanical properties, thermal stability and chemical inertness for a wide range of commercial and industrial application. To further extent its engineering uses, it is of great relevance to improve the mechanical performance of PEEK by reinforcing it with nanofillers [29].

However, few efforts have been made to investigate the thermal properties of the ceramic-based CNT nanocomposites. Hence, studying the thermal conductivity of ceramic-based nanocomposites comprising CNT is important. So, in this study, we tried to improve the mechanical properties without harming the thermal conductivity of MWCNT in the PEEK matrix, ZrO<sub>2</sub> coated MWCNT has been used. Zirconium dioxide (ZrO<sub>2</sub>) coated MWCNT has been prepared by two methods and compared with pristine MWCNT and virgin PEEK composites in terms of thermal properties were compared.

## 2. Experimental

### 2.1 Materials

The PEEK [unreinforced Poly (ether ether ketone)] (450G) has been purchased from DICT, Korea. This material is high performance thermoplastic and having melting point around 343 °C. The multi-walled carbon nanotube (MWCNT) prepared by chemical vapor deposition was purchased from ACN Tech. Co., Korea and purity is more than 95%. ZrOCl<sub>2</sub>.8H<sub>2</sub>O was employed as the precursor for the synthesis of ZrO<sub>2</sub> coating from Sigma-Aldrich, USA. Ethanol was purchased from Duksan Pure Chemicals Co. Ltd, Korea.

### 2.2 Processing of composites

#### 2.2.1 Making of MWCNT/ZrO<sub>2</sub> composites

Solid ZrOCl<sub>2</sub>.8H<sub>2</sub>O was first dissolved in 100 ml of distilled water to produce 0.2 mol/L solution under magnetic stirring. Then 30 mg of MWCNT without any pretreatment were added into the aqueous solution. After 30 min ultrasonic vibration, a black suspensions with MWCNT homogeneously dispersed were obtained. The stable aqueous suspension was then long drawn reflux condensed in a thermostatic water bath at the temperature of 100 °C, ensuring the isothermal hydrolyzing of ZrOCl<sub>2</sub>. Figure 1 shows the diagram of the hydrolysis process for the nanocomposites. During this hydrolytic process, the suspension was ultrasonicated for 10 min every 24 h to get a good dispersion of MWCNT in the aqueous solution. After approximately 72 h, the black suspension turned to gray. The advantage of hydrolyzation method is that shapes of formed nanotubes can be controlled by controlling those of isothermal hydrolyzation time. Some researchers [30] have already shown that if the hydrolyzation time increased with the reaction time, the thickness of the coating will be increased. So, we can control the shape of the nanotubes by controlling the reaction time. For comparison, a conventional chemical precipitation method was also used to prepare MWCNT/ZrO<sub>2</sub> nanocomposites. By ultrasonic vibration, 30 mg of MWCNT were homogeneously dispersed into 0.2 mol/L of ZrOCl<sub>2</sub>.8H<sub>2</sub>O aqueous solution to acquire the same stable black suspension. Under vigorous stirring, an appropriate amount of NH<sub>4</sub>OH was added drop by drop into the above 100 mL suspension. After that the whole mixture was further magnetically stirred for 60 min, a stable well-proportioned MWCNT/ZrO<sub>2</sub> nanocomposites suspension were obtained.

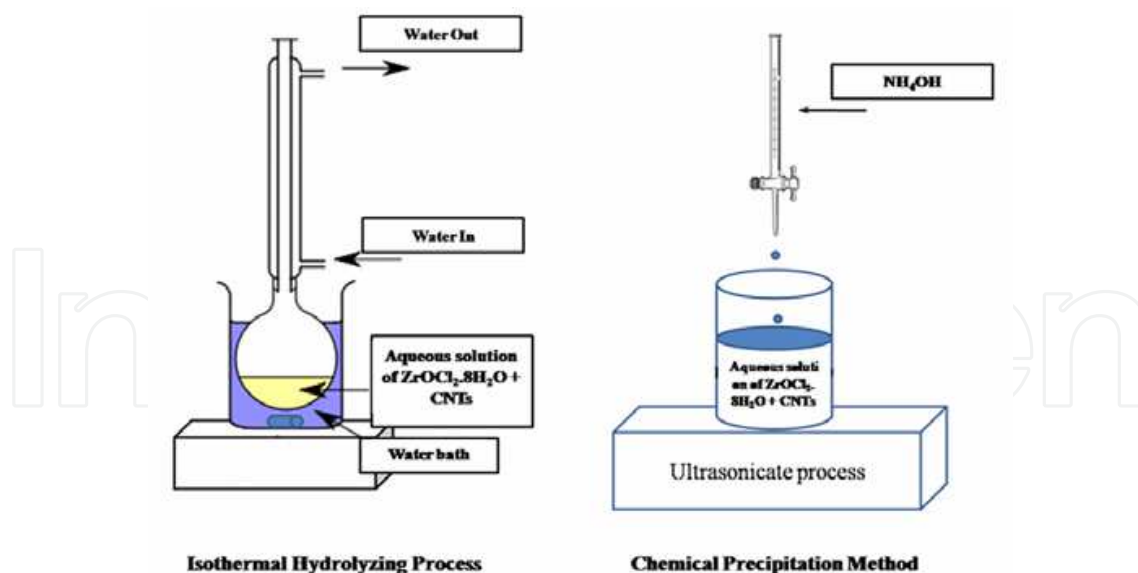


Fig. 1. A diagram of hydrolysis method and chemical precipitation methods for prepared nanocomposites

### 2.2.2 Making of PEEK/MWCNT composites and PEEK/ZrO<sub>2</sub> coated MWCNT composites

Brabender Plasticoder (Brabender Co.) has been used for preparation of PEEK/MWCNT composites and PEEK/ZrO<sub>2</sub> coated MWCNT composites. The mixing of sample carried out at 350 °C, 60 rpm for 5 min. Sample of four kinds was prepared. The sample having the code name, such as A, B, C and D for virgin EVA composites, PEEK/pristine MWCNT nanocomposites, PEEK/ZrO<sub>2</sub> coated MWCNT by isothermal process and PEEK/ZrO<sub>2</sub> coated MWCNT by chemical process, respectively and has been shown in Table 1.

Composition	Sample Code			
	A	B	C	D
	All are in wt%			
EVA	100	100	100	100
Pristine MWCNT	-	3	-	-
ZrO <sub>2</sub> coated MWCNT by isothermal process	-	-	3	-
ZrO <sub>2</sub> coated MWCNT by chemical process	-	-	-	3

Table 1. Compound formulations

### 2.3 XRD study

X-ray diffraction (XRD) experiment was carried out in D8 Advance, Bruker AXS (Germany) diffractometer with Cu-K $\alpha$  (wavelength of 0.14051 nm) and a monochromator on the diffracted beam. Experiment was performed at 40 kV of accelerating potential, 40 mA current, and a scanning rate of 5°min<sup>-1</sup>.

### 2.4 Dynamic mechanical analysis (DMA)

The dynamic mechanical properties of the samples were determined by using DMA Q800 (TA Instrument, Inc., USA) in tension mode. Rectangular film specimens were used for the

study. Samples were heated from room temperature to 280 °C at a heating rate of 10 °C/min in air atmosphere within impressed a frequency of 1 Hz.

### 2.5 Thermal conductivity measurement

DSC measurements were carried out using a TA Instruments Q-20 DSC instrument. The samples ( $\leq 10$  mg), sealed under aluminum pans were scanned in the temperature range of 30 to 400 °C. The heating rate is 10 °C min<sup>-1</sup> under the nitrogen atmosphere with a flow rate of 40 ml/min.

Heat flow measurement and heat capacity calculation by used DSC after thermal conductivity was calculated. First, equation (1) has been used to calculate the heat capacity ( $C_p$ ) of the composites.

$$C_p = (q/t) / (dt/t) = q / dt \quad (1)$$

where  $q$  is the heat flow difference between no sample and with sample,  $dt$  is the heating rate. Heat capacity ( $C_p$ ) was calculated at the three temperatures ( $T_g$ ,  $T_m$ ,  $T_c$ ) indicated by DSC and from the equation (2) thermal conductivity ( $\lambda$ ) of the composites was calculated.

$$\lambda = (8LC^2) / (C_p m d^2 p) \quad (2)$$

where  $L$  is sample thickness,  $C$  is apparent heat capacity (thick sample),  $C_p$  is the heat capacity,  $m$  is weight of the thick sample,  $d$  is sample diameter,  $p$  is oscillation period, 80 s [31].

### 2.6 TGA study

The equipment (Model TGA Q50), manufactured by TA Instrument, was used to test the samples. For TGA measurements, specimens were cut from the vulcanized samples as small pieces (5-10 mg). The specimens were heated from 30 to 650 °C at a constant increase in temperature (10 °C/min), in nitrogen atmosphere and the weight loss determined as a function of temperature.

### 2.7 AFM study

The atomic force microscopy was carried out using a Multimode SPM operated in AFM mode and manufactured by XE-100 (PSIA, Korea) at frequency 3 Hz and in non-contact mode.

### 2.8 Scanning electron microscopy (SEM)

The tensile fracture surface of the samples are scanned in a scanning electron microscope (JSM-6380LV of JEOL Co.; Acceleration voltage: 20kV) to study the dispersion of the MWCNTs in PEEK matrix. Samples are sputtered with gold-palladium prior to testing.

## 3. Results and discussion

XRD study is performed on the samples using WAXD machines. The change of composites crystallinity is measured on a Bruker AXS X-ray diffractometer (Germany). WAXD is used to observe the effect of pristine and ZrO<sub>2</sub> coated MWNTs content on the microstructure of pristine PEEK. Figure 2 describes the WAXD patterns for pristine PEEK and PEEK/MWNTs nanocomposites. Within a given range of scattering angles, four characteristic diffraction peaks appear at  $2\theta$  value of 18.82, 20.89, 22.84 and 28.92° respectively, which correspond to (100), (111), (200) and (211) reflections, respectively, the matrix orthorhombic unit cell [32].

This experiment confirms once again that the rate of crystallization of the matrix is influenced by the MWCNT types. A remarkable change from promotion to retardation is detected as the presence of wrapped MWCNTs. In contrast, no shift in the position of the Bragg reflections is observed, pointing out that all these composites present the same crystalline structure than pure PEEK. Samples incorporating pristine MWCNTs exhibit larger crystals than pure PEEK, whereas those with wrapped MWCNTs present similar or slightly lower crystal sizes. This behavior is also consistent with the results obtained from DSC analysis. This may be due to the better interaction between the MWCNTs and matrix surfaces resulting in improved adhesion between them at the interface which in turn favors the crystal growth mechanism. In the extreme case of the PEEK with ZrO<sub>2</sub> coated MWCNT composite, such effect is very clear.

It is also noteworthy that inter-planar distance corresponding to every peak position increases in the case of modified PEEK with MWCNTs, which again support the nucleating ability of nanotube into PEEK systems and support the results obtained from DSC study.

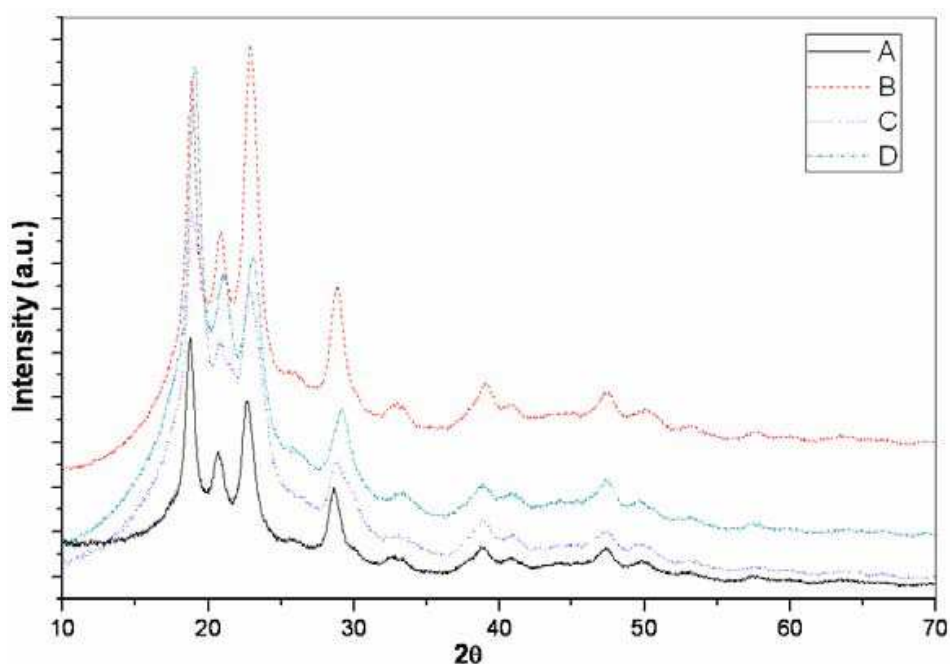
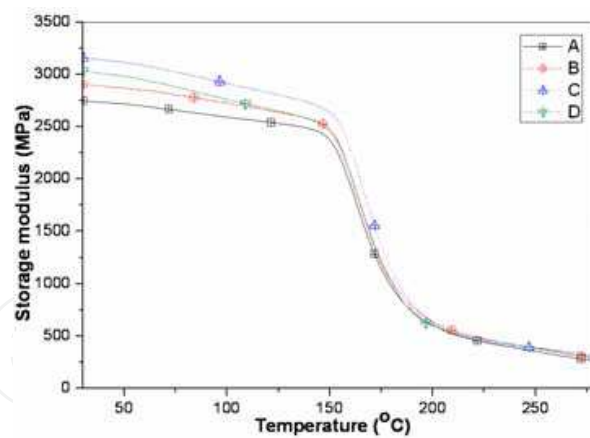
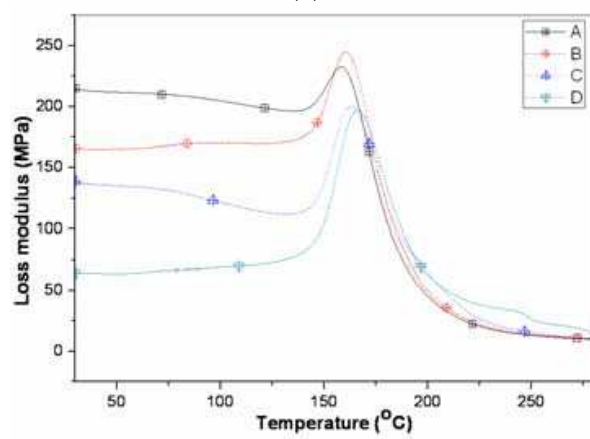


Fig. 2. XRD result of sample (A) PEEK, (B) PEEK/pristine MWCNT, (C) PEEK/ZrO<sub>2</sub> coated MWCNT by isothermal process, (D) PEEK/ZrO<sub>2</sub> coated MWCNT by chemical process

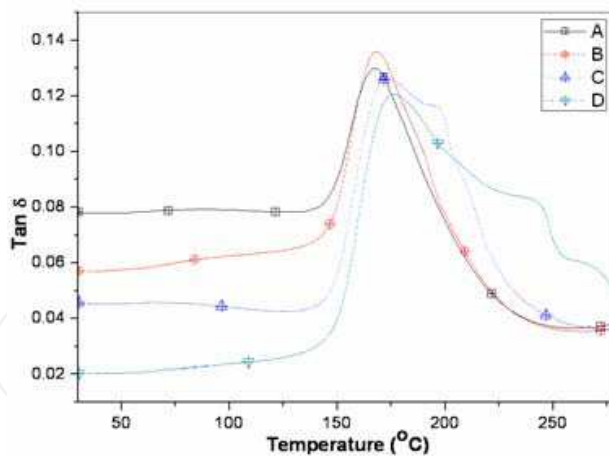
One of the major goals of employing ZrO<sub>2</sub> coated MWCNTs is to attain composites with enhanced mechanical properties, which ultimately determine the application of the material strength. The thermo-mechanical behavior of these composites was studied using dynamic mechanical analysis (DMA). Figure 3 shows, as an example, the dynamic mechanical spectra (storage modulus  $E'$ , loss modulus  $E''$  and  $\tan\delta$ ) as a function of temperature, at the frequency of 1 Hz, for PEEK and PEEK/MWCNT composites. It is evident that the storage modulus of the composites increases progressively with the addition of wrapped MWCNTs at temperatures below the glass transition, pointing out the stiffening effect of these MWCNTs. Therefore, the remarkable modulus enhancement observed in the PEEK/ZrO<sub>2</sub> wrapped MWCNTs composites should be attributed to a more effective load transfer from the matrix to the fillers likely resulting from the improved dispersing ability of the wrapped MWCNTs, combined with a stronger interfacial adhesion PEEK-MWCNT.



(a)



(b)



(c)

Fig. 3. (a) Storage modulus, (b) loss modulus and (c)  $\text{Tan}\delta$  result of sample (A) PEEK. (B) PEEK/pristine MWCNT, (C) PEEK/ $\text{ZrO}_2$  coated MWCNT by isothermal process, (D) PEEK/ $\text{ZrO}_2$  coated MWCNT by chemical process

On the other hand, our experimental data reveals a substantial drop in the storage modulus of all the samples between 160 and 180 °C, interval which corresponds to the glass transition of the materials. In this range, differences between  $E'$  of each composite and the matrix decrease considerably, and become insignificant at higher temperatures. The main reason is

the strong reduction of the load transfer efficiency in these composites as going through the glass transition.

The evolution of  $\tan\delta$  (ratio of the loss to storage modulus) as a function of temperature for PEEK and PEEK/ZrO<sub>2</sub> wrapped MWCNTs composites is shown in Fig. 3c. Several relaxation peaks can be observed: the maximum at lower temperatures ( $\beta$ -relaxation) is associated with local motions of the ketone groups [33], and the most intense peak (a relaxation) corresponds to the  $T_g$ . The incorporation of wrapped MWCNTs results in a small reduction of  $\tan\delta$  magnitude (a measure of the damping within the system) over the whole temperature range. With ZrO<sub>2</sub> coated MWCNTs, all relaxation peaks broaden and shift to the higher temperature side. This indicates that wrapped MWCNTs efficiently restrict the mobility of the PEEK chains, thereby increasing the stiffness of the matrix, which is reflected in higher transition temperatures [34].

DSC is performed on PEEK/MWCNT samples using a DSC 300 F3 (NETZSCH, Germany). Heat flow is monitored over the range of 30 to 400 °C with temperature modulation (+/- 0.8 °C every 60 sec) superimposed on a 10 °C/min heating and cooling rate under purge gas (nitrogen at 40 ml/min). The heating scan thermograms of PEEK and PEEK/ZrO<sub>2</sub>-MWNT nanocomposites are shown in Figure 4(a). The pristine PEEK samples produce a main melting peak at 340 °C. However, the addition of MWNTs the shoulder posterior to the main melting peak and an increase end point of the peak.

The addition of ZrO<sub>2</sub> coated MWCNTs also results in small variations of the melting temperature ( $T_m$ ) of the PEEK matrix (Figure 4a), showing similar trends to those observed from the cooling thermograms (Figure 4b). In the case of composites including 3 wt.% ZrO<sub>2</sub> coated MWCNTs dispersed in matrix,  $T_m$  increases ~5 °C, whereas for those incorporating 3 wt.% pristine MWCNT, it increases around ~2 °C than pristine PEEK. It is also important to notice that a small change in the specific heat associated to the glass transition of the matrix in the composites can be visualized in the heating thermograms. The incorporation of ZrO<sub>2</sub> coated MWCNTs dispersed in the matrix shift this transition towards higher temperatures this phenomenon has been proved by DMA measurements.

The thermal conductivity of PEEK composites has been measured from the DSC study and is depicted in Table 2. The thermal conductivity of the composites has been measured in three different temperature zones, namely  $T_g$ ,  $T_c$  and  $T_m$ . It has been that thermal conductivity also rises progressively with increasing temperature, as shown in Table 2, being the increment in comparison to the pure matrix (0.22 W/mK). Also, it can be seen that composites loaded with ZrO<sub>2</sub> coated MWCNTs present higher values, indicating that the thermal conductivity is also sensitive to the attributes of the filler, presence of defects and content in metal impurities. ZrO<sub>2</sub> coated MWCNTs samples display slightly lower thermal conductivity than pristine MWCNTs composite, since the wrapping hinders the direct contact among the tubes. Taking into account the exceptionally high thermal conductivity of chemically treated ZrO<sub>2</sub> coated MWCNTs (0.43 W/mK), the improvements in thermal conductivity observed in these composites are more than isothermally treated ZrO<sub>2</sub> coated MWCNTs those expected according to the rule of mixtures. The main reason for this behavior is the coating of the Zr on the MWCNTs. While coating the chemical process is so first that all the MWCNTs are not wrapped by the Zr rather than isothermal process which is slow and steady process. We have already discussed about this in our previous literature [35]. Also, this discrepancy could be attributed to the small thermal conductance of the nanotube-polymer interface and the high interfacial thermal resistance between MWCNTs [36], which limit considerably the heat transfer. Also, it will be quite obvious that thermal conductivity will be higher for the pristine MWCNTs rather than coated MWCNTs.



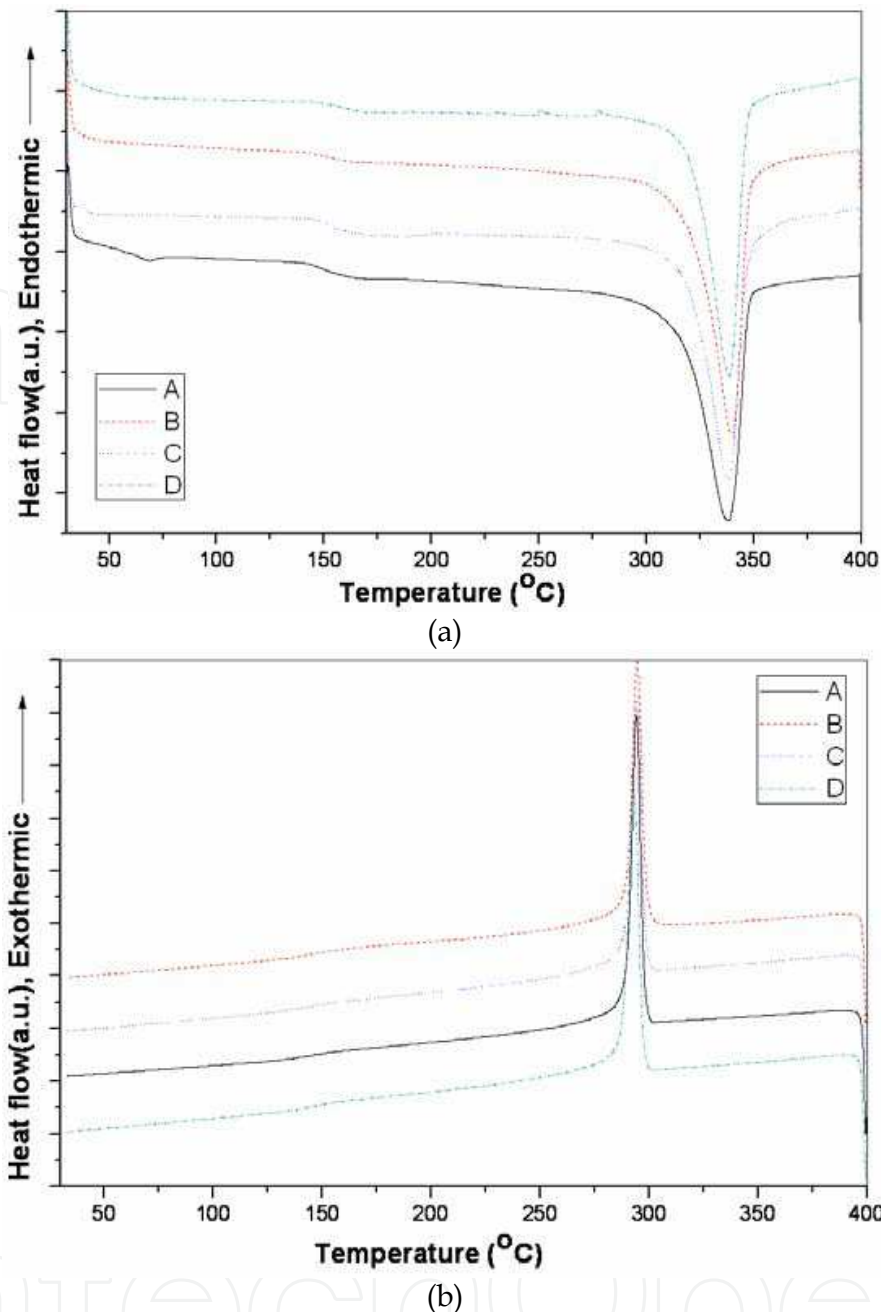


Fig. 4. (a) Endotherm and (b) exotherm result of the composites (A) PEEK, (B) PEEK/pristine MWCNT, (C) PEEK/ $ZrO_2$  coated MWCNT by isothermal process, (D) PEEK/ $ZrO_2$  coated MWCNT by chemical process

Thermogravimetric analysis (TGA Q500, TA Instruments) is carried out to study the thermal stability of each PEEK/MWCNTs nanocomposite from room temperature to 800 °C at a heating rate of 10 °C/min under purge gas (nitrogen at 40 ml/min). Figure 5 shows the TGA thermograms of PEEK with  $ZrO_2$  coated MWCNTs composites. The thermo-degradation of PEEK and PEEK nanocomposites takes place in one step. The onset degradation temperature of PEEK is around 580 °C but with the addition of pristine MWCNTs and  $ZrO_2$  coated MWCNTs the onset degradation temperature increases. This step of the thermal degradation also takes place at a higher temperature side in the presence of MWCNTs. This

Properties	Sample code				
	A	B	C	D	
T <sub>g</sub> (°C)	143.66	147.05	154.17	157.55	
T <sub>m</sub> (°C)	338.14	339.84	338.48	338.48	
T <sub>c</sub> (°C)	294.10	294.44	294.44	293.08	
C <sub>p</sub> (J/g °C)	T <sub>g</sub>	0.0640	0.0630	0.0614	0.0606
	T <sub>m</sub>	0.0081	0.0103	0.0074	0.0081
	T <sub>c</sub>	0.0037	0.0184	0.0148	0.0155
Thermal conductivity (W/mK)	T <sub>g</sub>	0.22	0.23	0.22	0.22
	T <sub>m</sub>	0.23	0.39	0.30	0.37
	T <sub>c</sub>	0.27	0.45	0.39	0.43

Table 2. Heat capacity and thermal conductivity of the composites (A) PEEK. (B) PEEK/pristine MWCNT, (C) PEEK/ZrO<sub>2</sub> coated MWCNT by isothermal process, (D) PEEK/ZrO<sub>2</sub> coated MWCNT by chemical process

region is highly dependent on the types of MWCNTs because the mass loss becomes higher with ZrO<sub>2</sub>/MWCNT by isothermal hydrolyzing. On the other hand, Figure 5 also suggests that the MWCNT has a good affinity to the PEEK region in the PEEK/MWCNT nanocomposites, indicating that the MWCNT is dominantly dispersed in the PEEK matrix. As the MWCNT region being increases, thermal properties of the PEEK/MWCNT nanocomposites have been enhanced because the MWCNT possesses good thermal properties. This behavior could be explained by the presence of the char formed from PEEK matrix during the degradation step, which is further stabilized through  $\pi$ - $\pi$  electronic interactions with the coated nanotubes [37].

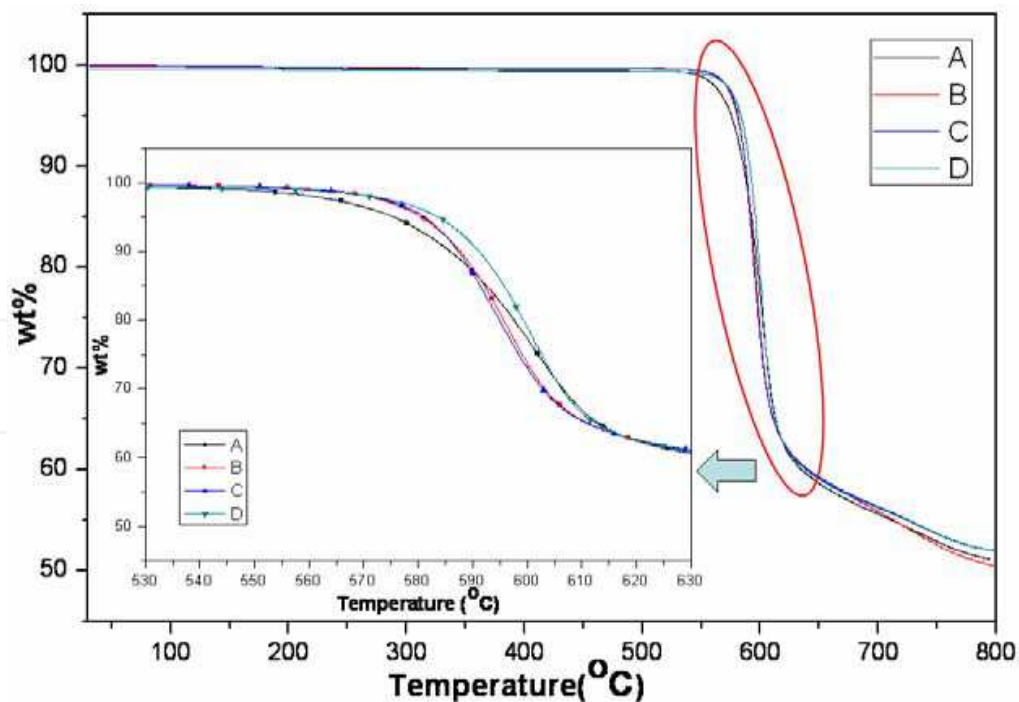


Fig. 5. TGA result of the composites (A) PEEK. (B) PEEK/pristine MWCNT, (C) PEEK/ZrO<sub>2</sub> coated MWCNT by isothermal process, (D) PEEK/ZrO<sub>2</sub> coated MWCNT by chemical process

In the present study AFM is also used to study the microstructure of fluoroelastomer/MWCNT samples. From the figure it can be observed that the topographical image of PEEK and PEEK/MWCNTs composite are not as clear as has been observed in other nanotube/polymer composites. However, it is generally known that it is not easy to separate the magnetic contrast from other background forces in MFM topography images. But polymer/nanotube composites are two phase materials with two distinct magnetic properties. The nanotubes are paramagnetic or diamagnetic depending upon their orientation whereas the polymer matrix is paramagnetic. Interpretation of an observed image usually relies on the understanding of micromagnetism.

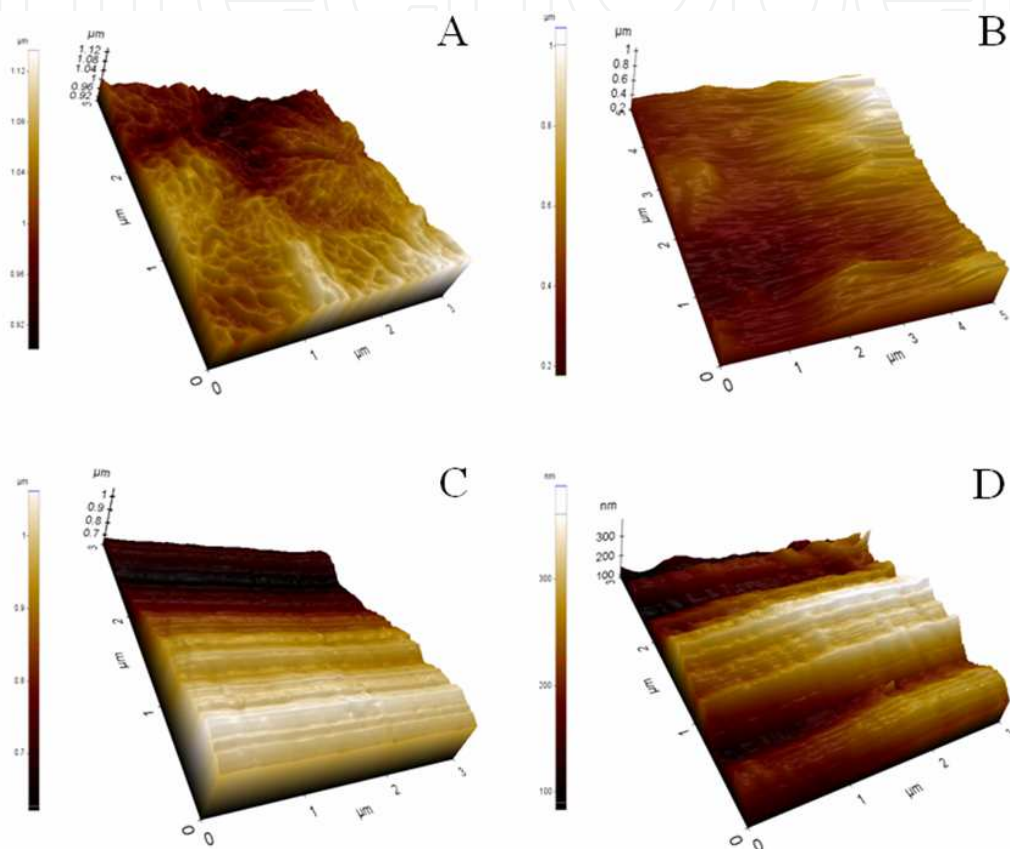


Fig. 6. AFM images of sample (A) PEEK, (B) PEEK/pristine MWCNT, (C) PEEK/ZrO<sub>2</sub> coated MWCNT by isothermal process, (D) PEEK/ZrO<sub>2</sub> coated MWCNT by chemical process

The homogeneous dispersion of the MWCNTs in the polymer matrix is one of the most important features for reinforcing the composites, since any heterogeneity or aggregation could result in structural defects, which would have detrimental effects on the mechanical properties. A Field Emission Scanning Electron Microscopy (FE-SEM) is performed to observe the morphology of the cryo fractured surfaces (fractured by mechanical force) of PEEK/MWCNT nanocomposites. Figure 7a, is can be observed the furrow like structure of the virgin PEEK matrix. In Figure 7b, MWCNTs (which appear as bright spots) are quite agglomerated, forming a highly entangled interconnected structure. In contrast, for all the ZrO<sub>2</sub> coated MWCNT composites analyzed, the nanofillers are found to be randomly and well-dispersed within the matrix by the shear force from melt-blending (Figure 7c and 7d). No MWCNT agglomerations or entanglements were observed in the whole examined areas;

the energy of the shear force process breaks up the aggregates, leading to a fine dispersion of the coated MWCNTs, which results in a large MWCNT-matrix effective contact area. Moreover, no open ring holes or voids were found around the MWCNTs, hinting at the existence of good filler-matrix interfacial adhesion.

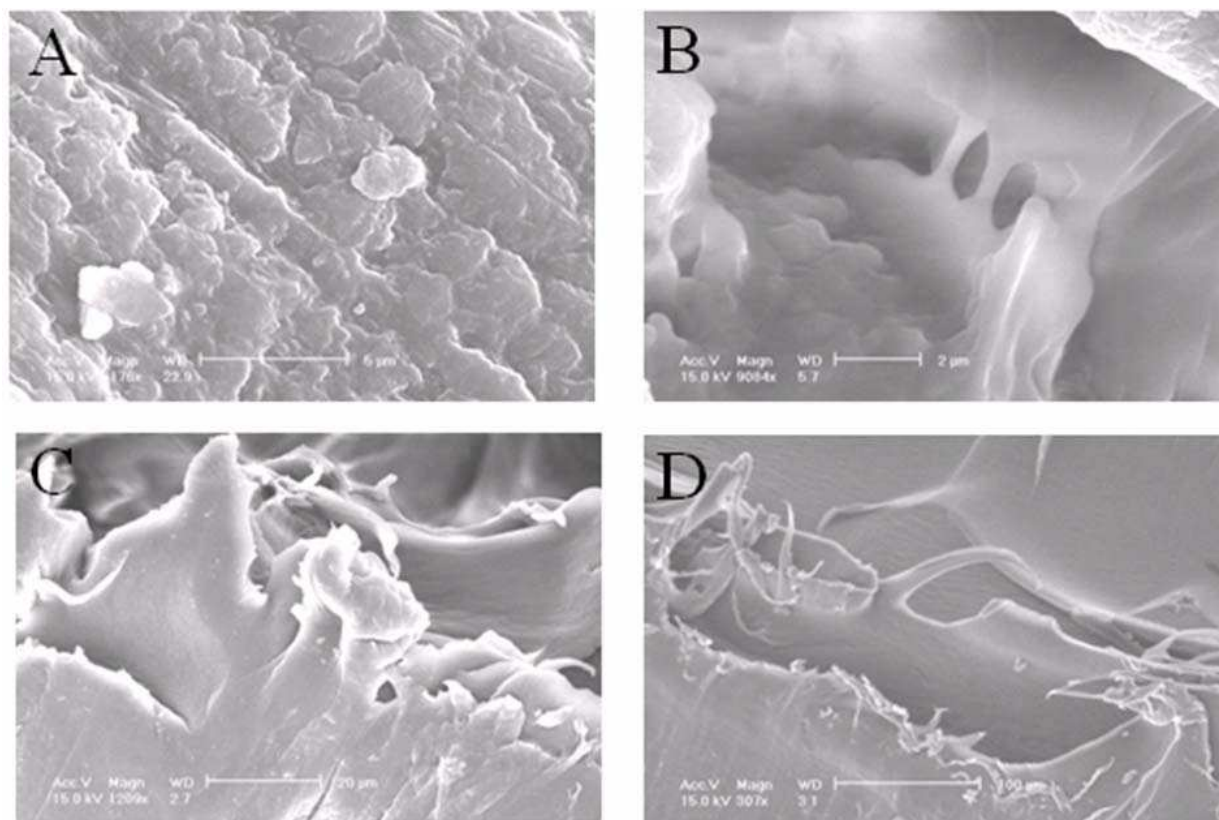


Fig. 7. FESEM images of composite (A) PEEK, (B) PEEK/pristine MWCNT, (C) PEEK/ZrO<sub>2</sub> coated MWCNT by isothermal process, (D) PEEK/ZrO<sub>2</sub> coated MWCNT by chemical process

#### 4. Conclusion

The structure, morphology and thermal properties of high performance semicrystalline PEEK/MWCNT composites incorporating two differently coated MWCNTs have been characterized. X-ray diffraction patterns of the ZrO<sub>2</sub> coated MWCNTs dispersed in the polysulfones revealed an effective debundling and disentanglement of the MWCNTs. TGA thermograms demonstrated a remarkable increase in the degradation temperatures of the composites by the incorporation of the ZrO<sub>2</sub> coated MWCNT. Also, it has been found that thermal conductivity of the chemical treated ZrO<sub>2</sub> coated MWCNT is more good than isothermal treated ZrO<sub>2</sub> coated MWCNT. Scanning electron microscopy observations showed that the wrapped MWCNTs were homogeneously dispersed in the thermoplastic matrix using a conventional melt-extrusion process.

#### 5. Acknowledgement

This work was supported by BK-21 fellowship offered to the author from I-Cube Centre, Gyeongsang National University. The authors acknowledge the instrumental and technical

support provided by Department of Polymer Science and Engineering, Gyeongsang National University, Republic of Korea.

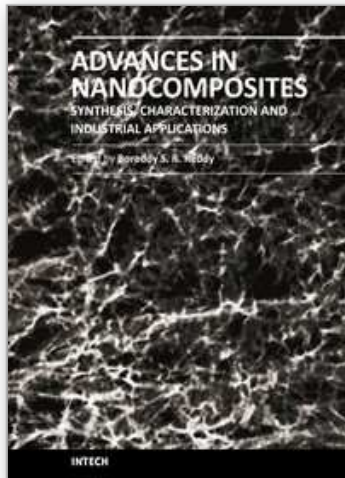
## 6. References

- [1] Iijima, S (1991) Helical microtubules of graphitic carbon. *Nature* 354: 56-58.
- [2] Baughman RH, Zakhidov AA, de Heer WA (2002) Carbon nanotubes--the route toward applications. *Science* 297: 787-92.
- [3] Dai H (2002) Carbon nanotubes: opportunities and challenges. *Surf. Sci.* 500: 218-41.
- [4] Lupo F, Kamalakaran R, Scheu C, Grobert N, Ruhle M (2004) Microstructural investigations on zirconium oxide-carbon nanotube hybrid materials synthesized by hydrothermal crystallization. *Carbon* 42:1995-99.
- [5] Zhu L, Sun Y, Hess DW, Wong CP (2006) Well-Aligned Open-Ended Carbon Nanotube Architectures: An Approach for Device Assembly. *Nano Lett.* 6: 243-47.
- [6] Chan RHM, Fung CKM, Li WJ (2004) Rapid assembly of carbon nanotubes for nanosensing by dielectrophoretic force. *Nanotechnology* 15: S672-S677.
- [7] Yang S, Song H, Chen X, Okotrub AV, Bulusheva LG (2007) Electrochemical performance of arc-produced carbon nanotubes as anode material for lithium-ion batteries. *Electrochim. Acta* 52: 5286-93.
- [8] Ding MQ, Shao WS, Li XH, Bai GD, Zhang FQ, Li HY, et al. (2005) Approach for fabricating microgated field-emission arrays with individual carbon nanotube emitters. *J. Appl. Phys. Lett.* 87: 233118.
- [9] Guo DJ, Li HL (2005) Highly dispersed Ag nanoparticles on functional MWCNT surfaces for methanol oxidation in alkaline solution. *Carbon* 43: 1259-64.
- [10] Felten A, Bittencourt C, Pireaux JJ (2006) Gold clusters on oxygen plasma functionalized carbon nanotubes: XPS and TEM studies. *Nanotechnology* 17: 1954-59.
- [11] Liu SW, Wehmschulte RJ (2005) A novel hybrid of carbon nanotubes/iron nanoparticles: iron-filled nodule-containing carbon nanotubes. *Carbon* 43: 1550-55.
- [12] Wang YH, Li YN, Lu J, Zang JB, Huang H (2006) Microstructure and thermal characteristic of Si-coated multi-walled carbon nanotubes. *Nanotechnology* 17: 3817-21.
- [13] Fu L, Liu ZM, Liu YQ, Han BX, Wang JQ, Hu PA, et al (2004) Coating Carbon Nanotubes with Rare Earth Oxide Multiwalled Nanotubes. *Adv. Mater.* 16: 350-52.
- [14] Korneva G, Ye HH, Gogotsi Y, Halverson D, Friedman G, Bradley JC, et al (2005) Carbon Nanotubes Loaded with Magnetic Particles. *Nano Lett.* 5: 879-84.
- [15] Jitianu A, Cacciaguerra T, Benoit R, Delpeux S, Beguin F, Bonnamy S (2004) Synthesis and characterization of carbon nanotubes-TiO<sub>2</sub> composites. *Carbon* 42: 1147-51.
- [16] Farmer DB, Gordon RG (2006) Atomic Layer Deposition on Suspended Single-Walled Carbon Nanotubes via Gas-Phase Noncovalent Functionalization. *Nano Lett.* 6: 699-703.
- [17] Lee SM, Oh SH, Cho W I, Jang H (2006) The effect of zirconium oxide coating on the lithium nickel cobalt oxide for lithium secondary batteries. *Electrochim. Acta* 52: 1507-13.

- [18] Zhu LQ, Fang Q, He G, Liu M, Zhang LD (2005) Microstructure and optical properties of ultra-thin zirconia films prepared by nitrogen-assisted reactive magnetron sputtering. *Nanotechnology* 16: 2865-69.
- [19] Chen YY, Wei WJ (2006) Processing and characterization of ultra-thin yttria-stabilized zirconia (YSZ) electrolytic films for SOFC. *Solid State Ionics* 177: 351-57.
- [20] Sakhno OV, Goldenberg LM, Stumpe J, Smirnova TN (2007) Mechanical testing of pyrolysed poly-furfuryl alcohol nanofibres. *Nanotechnology* 18: 105704.
- [21] Eslamian M, Ahmed M, Ashgriz N (2006) Modelling of nanoparticle formation during spray pyrolysis. *Nanotechnology* 17: 1674-85.
- [22] Ohtsu Y, Hino Y, Misawa T, Fujita H, Yukimura K, Akiyama M (2007) Influence of ion-bombardment-energy on thin zirconium oxide films prepared by dual frequency oxygen plasma sputtering. *Surf. Coat. Technol.* 201: 6627-30.
- [23] Chang SM, Doong RA (2005) ZrO<sub>2</sub> thin films with controllable morphology and thickness by spin-coated sol-gel method. *Thin Solid Films* 489: 17-22.
- [24] Neagu R, Perednis D, Princivalle A, Djurado E (2006) Zirconia coatings deposited by electrostatic spray deposition A chemical approach. *Solid State Ionics* 177: 1451-60.
- [25] Alexandrou I, Kymakis E, Amaratunga GAJ (2002) Polymer-nanotube composites: Burying nanotubes improves their field emission properties. *Appl. Phys. Lett.* 80: 1435-37.
- [26] Bryning MB, Milkie DE, Islam MF, Kikkawa JM, Yodh AG (2005) Thermal conductivity and interfacial resistance in single-wall carbon nanotube epoxy composites. *Appl. Phys. Lett.* 87: 161909-12.
- [27] Biercuk MJ, Llaguno MC, Radosavljevic M, Hyun JK, Johnson AT, Fischer JE (2002) Carbon nanotube composites for thermal management. *Appl. Phys. Lett.* 80: 2767-69.
- [28] Zhan G-D, Kuntz JD, Garay JE, Mukherjee AK (2003) Electrical properties of nanoceramics reinforced with ropes of single-walled carbon nanotubes. *Appl. Phys. Lett.* 83: 1228-30.
- [29] Diez-Pascual AM, Naffakh M, Gonzalez-Dominguez JM, Anson A, Martinez-Rubi Ya, Martinez MT, Simard B, Gómez MA (2010) High performance PEEK/carbon nanotube composites compatibilized with polysulfones-II. Mechanical and electrical properties. *Carbon* 48: 3500-11.
- [30] Lu Y, Zang JB, Shan SX, Wang YH (2008) Synthesis and Characterization of Core-Shell Structural MWNT-Zirconia Nanocomposites. *Nano Lett.* 8: 4070-74.
- [31] ASTM E1958-98. Thermal conductivity and thermal diffusivity by modulated temperature differential scanning calorimetry.
- [32] Rols S, Righi A, Alvarez L, Anglaret E, Almairac R, Journet C, et al. Diameter distribution of single wall carbon nanotubes in nanobundles. *Eur Phys J B* 2000;18(2):201-6.
- [33] Cebe P, Chung SY, Hong SD. Effect of thermal history on mechanical properties of poly(ether ether ketone) below the glass transition temperature. *J Appl Polym Sci.* 1987;33(2):487-503.
- [34] Diez-Pascual AM, Naffakh M, Gonzalez-Dominguez JM, Anson A, Martinez-Rubi Y, Martinez MT, Simard B, Gomez MA (2010), High performance PEEK/carbon

- nanotube composites compatibilized with polysulfones-I. Structure and thermal properties. *Carbon* 48, 3485 – 3499.
- [35] K. Pal, D. J. Kang, Z. X. Zhang, J. K. Kim (2010), Synergistic Effects of Zirconia-Coated Carbon Nanotube on Crystalline Structure of Polyvinylidene Fluoride Nanocomposites: Electrical Properties and Flame-Retardant Behavior, *Langmuir*, 26(5), 3609–3614.
- [36] Nan C-W, Liu G, Lin Y, Li M (2004), Interface effect on thermal conductivity of carbon nanotube composites. *Appl Phys Lett*, 85: 3549–51.
- [37] Peeterbroeck, S.; Laoutid, F.; Taulemesse, J.-M.; Monteverde, F.; Lopez-Cuesta, J.-M.; Nagy, J. B.; Alexandre, M.; Dubois, P. *Adv. Funct. Mater.* 2007, 17, 2787.

IntechOpen



## **Advances in Nanocomposites - Synthesis, Characterization and Industrial Applications**

Edited by Dr. Boreddy Reddy

ISBN 978-953-307-165-7

Hard cover, 966 pages

**Publisher** InTech

**Published online** 19, April, 2011

**Published in print edition** April, 2011

Advances in Nanocomposites - Synthesis, Characterization and Industrial Applications was conceived as a comprehensive reference volume on various aspects of functional nanocomposites for engineering technologies. The term functional nanocomposites signifies a wide area of polymer/material science and engineering, involving the design, synthesis and study of nanocomposites of increasing structural sophistication and complexity useful for a wide range of chemical, physicochemical and biological/biomedical processes. "Emerging technologies" are also broadly understood to include new technological developments, beginning at the forefront of conventional industrial practices and extending into anticipated and speculative industries of the future. The scope of the present book on nanocomposites and applications extends far beyond emerging technologies. This book presents 40 chapters organized in four parts systematically providing a wealth of new ideas in design, synthesis and study of sophisticated nanocomposite structures.

### **How to reference**

In order to correctly reference this scholarly work, feel free to copy and paste the following:

Kaushik Pal and Jin Kuk Kim (2011). Thermal Conductivity Improvement of PEEK/ZrO<sub>2</sub> Coated MWCNT Nanocomposites, *Advances in Nanocomposites - Synthesis, Characterization and Industrial Applications*, Dr. Boreddy Reddy (Ed.), ISBN: 978-953-307-165-7, InTech, Available from:

<http://www.intechopen.com/books/advances-in-nanocomposites-synthesis-characterization-and-industrial-applications/thermal-conductivity-improvement-of-peek-zro2-coated-mwcnt-nanocomposites>

**INTECH**  
open science | open minds

### **InTech Europe**

University Campus STeP Ri  
Slavka Krautzeka 83/A  
51000 Rijeka, Croatia  
Phone: +385 (51) 770 447  
Fax: +385 (51) 686 166  
[www.intechopen.com](http://www.intechopen.com)

### **InTech China**

Unit 405, Office Block, Hotel Equatorial Shanghai  
No.65, Yan An Road (West), Shanghai, 200040, China  
中国上海市延安西路65号上海国际贵都大饭店办公楼405单元  
Phone: +86-21-62489820  
Fax: +86-21-62489821



© 2011 The Author(s). Licensee IntechOpen. This chapter is distributed under the terms of the [Creative Commons Attribution-NonCommercial-ShareAlike-3.0 License](#), which permits use, distribution and reproduction for non-commercial purposes, provided the original is properly cited and derivative works building on this content are distributed under the same license.

IntechOpen

IntechOpen